

CONDENSATION PROCESSES IN THE EARLY SOLAR NEBULA - EXPERIMENTAL APPROACHES.

A. KROPF¹ and G. LIBOUREL^{1,2}, ¹CRPG-CNRS, 15, Rue Notre-Dame des Pauvres, BP20, 54501 Vandoeuvre les Nancy, France, (akropf@crpg.cnrs-nancy.fr) ²ENSG-INPL, BP40, 54501 Vandoeuvre les Nancy, France.

Introduction: Type-A Calcium-Aluminium-rich inclusions (CAIs) in some meteorites often have a zonal structure with corundum (Al_2O_3) in the center and phases like Hibonite ($\text{CaAl}_{12}\text{O}_{19}$) and Grossite (CaAl_4O_7) towards the rims. This observed mineralogical sequence is similar to a theoretically calculated formation sequence for assumed solar conditions, that is based on fractionary crystallization: the “full condensation code” [1, 2]. Due to the highly refractory character of Ca- and Al-rich phases, CAIs are interpreted to represent the first solid matter of the young solar system [3]. These first particles are thought to have formed in a hot, reducing environment during the cooling of the initial solar molecular cloud [3]. However, it is still unclear if these early condensates were formed under fractionated or equilibrated conditions. Questions of the kinetics and the precise nature of these processes (homogeneous / heterogeneous condensation) have still to be answered as well.

In order to explore details of these processes we developed an experimental device to study high temperature/low pressure condensation from a gas with a CMAS chemistry and solar or CAI-like element ratios. The main goal of this project is to get data from in-situ and post-mortem measurements of newly formed condensates, an experimental condensation sequence and finally an experimental proxy of the young stellar environment.

Methods: The primary idea of the new experiments is based on previous work of [4], which used laser ablation techniques to get a gas of solar composition for high temperature condensation experiments.

The new experimental setup provides higher experimental temperatures (<1800 K) and has improved abilities to tune, control and reproduce the chosen experimental pressures and temperatures. Furthermore, to control the oxygen fugacity, gases like CO, CO₂, Ar, etc., can be added in small quantities and sensitively enough to keep the total pressure and temperature sufficiently constant.

The setup (**Fig. 1**) consists of two vacuum chambers which are vertically connected by a tube. These chambers can be evacuated by two independent vacuum pumping systems (turbo-molecular/primary pumps). The lower and larger main chamber contains a series of four vertically fixed graphite tube furnaces that surround a thin alumina tube (inner diameter 4 mm). The bottom of this tube ends a few millimeters above a rotating glass target for an UV laser. This piece of glass has a CMAS composition with solar

element ratios (54 wt.% SiO₂, 4 wt.% Al₂O₃, 39 wt.% MgO and 3 wt.% CaO) or CAI-like element ratios (28 wt.% SiO₂, 35 wt.% Al₂O₃, 7 wt.% MgO and 30 wt.% CaO). Interaction of the laser beam with the target produces a plasma/gas with the desired composition. This gas enters the thin alumina tube at the bottom.

The four furnaces are used to produce a certain temperature profile in the alumina tube. To control the temperatures, S-type thermocouples are used. External thermocouples are fixed very close to the furnaces, but outside of the alumina tube. Another thermocouple can be inserted and moved inside of the tube. It records a profile of the real temperatures in the tube under experimental conditions. These data are used to get calibration curves for the external thermocouples. The internal thermocouple has to be removed for all experiments. Currently, temperatures can reach 1800 K in each furnace. The top of the alumina tube ends very close to the bottom end of another, bigger vertical alumina tube that leads directly to the second vacuum chamber.

An experiment starts by evacuating the entire system to $P \approx 10^{-6}$ mbar. After switching off the turbo pump at chamber 1, this chamber is evacuated only through the alumina tube(s), chamber 2 and finally the pump for chamber 2. The experimental condensation pressure is equal to the pressure in chamber 1. By controlling the pump power for chamber 2, vacuum condensation experiments can be done in the range within $1 \text{ mbar} > P_{\text{exp}} > 10^{-5}$ mbar. After the furnaces have been brought to experimental temperatures the UV-laser is activated. Gas particles are produced by shock cooling of the ablation plasma and forced to enter the alumina tube. They pass the first furnace (F1) with a temperature maximum (1600-1800 K), causing a re-homogenization of the gas. The second and third furnaces (F2 & F3) provide the desired condensation temperature over a distance of several millimeters between them. Furnace 4 (F4) ensures a symmetry of the entire temperature profile (see **Fig. 1** and **2**).

For post-mortem experiments we collect condensates by fixing a sample collector (Pt, Mo, Ni or Cu grid) inside of the alumina tube in the condensation zone between furnace 2 and 3. Condensates are analysed by TEM and SEM/FEG-SEM.

For in-situ experiments, the entire device can be installed into a beamline at the European Synchrotron Radiation Facility (ESRF) in Grenoble, France. In situ diffraction data (using SAXS and WAXS techniques)

of newly formed condensates can provide information about mineralogy, grain size distribution and kinetics.

Preliminary Results: We report on first condensation experiments using a gas with CAI-like glass target composition and we present preliminary TEM post mortem characterisation data.

Experiment e156 was done at $P = 1 \cdot 10^{-4}$ mbar and with the condensation temperature $T_{\text{cond}} = 1343$ K. Experiment e158 was done at $P = 2 \cdot 10^{-4}$ mbar and $T_{\text{cond}} = 1473$ K. The homogenization temperature (at furnace F1) was $T_{\text{H}} = 1600$ K, the time of laser-target interaction lasted 120 minutes and the oxygen fugacity was close to the C/CO buffer. TEM analysis of collected particles were done and are in progress. Mineral phases are identified on the bases of atomic ratio diagrams.

After proceeding e156, fourteen particles on the grid could be analysed by TEM. Almost all of them show the filament-like shape of a whisker (**Fig. 3a, 3b**) with a typical length of about 300 nanometers and a thickness of about 30-100 nanometers. Others have rounded, drop-like shapes, but all are identified as crystalline matter. The mineralogical compositions are close to melilite. Several results plot directly on the melilite solid solution line between the endmembers åkermanite ($\text{Ca}_2\text{MgSi}_2\text{O}_7$) and gehlenite ($\text{Ca}_2\text{Al}(\text{AlSi})\text{O}_7$) with $\text{Ak}_{60} - \text{Ak}_{100}$.

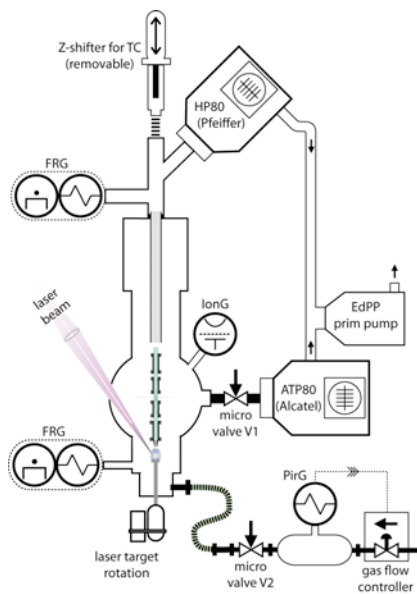


Fig. 1: Experimental setup (not scaled). Abbrev: IonG, FRG = vacuum gauges; HP80, ATP80, EdPP = vacuum pumps;

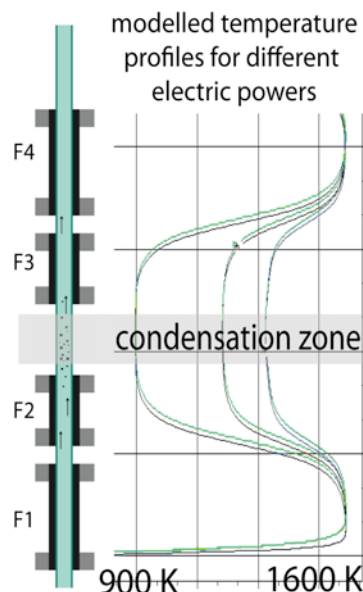


Fig. 2: Calculated temperature profile inside the alumina tube. The temperature modeling was done by A. DEGIOVANNI, ENSEM, Nancy (France).

Experiment e158 provided thirteen particles with sizes of 200-300 nanometer. Crystals with rounded shapes dominate (**Fig. 3c, 3d**). Two different phases were identified: most samples plot close to the melilite endmember gehlenite ($\text{Ca}_2\text{Al}(\text{AlSi})\text{O}_7$), three others close to grossite (CaAl_4O_7). Corundum was not found and most e158 samples are Mg-free.

The composition, monocrystalline structure and the whisker shape of condensates lead to the conclusion that under given experimental conditions only condensation out of a gas can produce these crystals. Laser ablation ejecta are excluded.

These first results show that the new experimental setup is basically working and that we can start to proceed more experiments using solar gas compositions and with solar nebula conditions. More results will be presented at the conference talk.

[1] Petaev, M. I. & Wood, J. A. (2005) ASP Conf. Ser. , Vol 341, 373-406. [2] Ebel, D. & Grossman, L. (2000) *GCA*, 64(2), 339-366. [3] Amelin, Y. et al. (2002) *Sci*, 297, 1678-1683. [4] Toppani, A. et al. (2006) *GCA*, 70, 5035-5060.

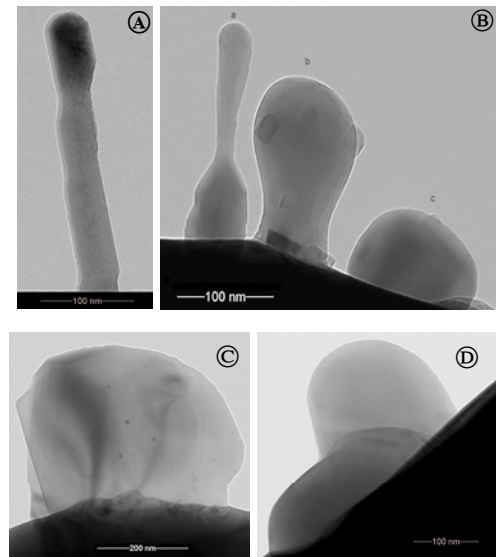


Fig. 3a, 3b: condensates from exp156, plotting on the melilite solid solution line.

Fig. 3c, 3d: condensates from exp158, identified as gehlenite (c) and grossite (d).